Proceedings of the 5th ECPMG 2024
5th European Conference on Physical Modelling in Geotechnics
2-4 October 2024, Delft, the Netherlands

An investigation into the effects of pile stiffness on pile working load capacity in clay utilising novel modelling techniques

G. Sabaliauskaite
Department of Civil Engineering, City, University of London, UK, greta.sabaliauskaite@city.ac.uk

S. Divall, A.M. McNamara, S.E. Stallebrass, R.N. Taylor
Department of Civil Engineering, City, University of London, UK
sam.divall@city.ac.uk, a.mcnamara@city.ac.uk, s.e.stallebrass@city.ac.uk, r.n.taylor@city.ac.uk

ABSTRACT: The rapid expansion of cities is driving the need to develop piled foundations which are able to support increasingly larger loads for the construction of high-rise buildings. Current research on piled foundations has focused on methods of reducing the size of piles whilst maintaining or increasing their capacity in an attempt to conserve the limited amount of underground space available. Generally, the ultimate capacity of a pile is achieved through shaft friction between the pile and the soil. The amount of undrained shear strength, s_u, of a soil that is mobilised by a pile shaft depends on the adhesion factor, α. For bored piles in clay, α varies between 0.35-0.50, suggesting that a large proportion of s_u along the pile shaft length is not mobilised. Recent research suggests that piles with a lower stiffness increase the proportion of s_u mobilised by allowing the pile to strain within the soil. Therefore, it would be beneficial to have a better understanding of the soil-pile interaction of lower stiffness piles in order to achieve higher working load capacities. A series of geotechnical centrifuge tests were undertaken on piles with varying axial stiffness in order to investigate this phenomenon. The tests were conducted at 50*g* at City, University of London, investigating the displacement of the piles under applied axial load.

1 INTRODUCTION

Piled foundations generate their capacity from end bearing and shaft resistance, and for the required mobilisation to occur, settlement of the pile is also necessary. Both end bearing and shaft resistance capacities are dependent on the undrained shear strength, S_u, of the fine grained soil in which the pile is installed in. During pile design, the proportion of S_u mobilised is typically governed by bearing coefficients N_c and α, where N_c is the end bearing coefficient and α is the pile shaft adhesion factor. These coefficients are dependent not only on the installation method of the pile but also its geometry.

2 BACKGROUND

The development and expansion of cities is inevitably leading to the use of increasingly larger piles which are necessary in supporting the construction of high-rise buildings. However, as most cities already have congested underground systems which carry electric cables, gas mains, transport links, water and sewage services, the space necessary to build ever-larger foundations is becoming sparse.

In order to mobilise the shaft and base resistance, some displacement of the pile is necessary. This is particularly true for bored piles installed in fine-grained soils, such as clay, as they typically achieve their capacity through skin friction. Therefore, it is essential to investigate the effect of stiffness on pile capacity.

In a study by Panchal *et al.*, (2019), a preliminary centrifuge test was conducted which investigated the performance of a low stiffness pile relative to that of a conventional, high stiffness pile. It was reported that the pile with a lower stiffness did in fact displace and strain along the length of the pile shaft by a greater degree, thus mobilising a larger proportion of skin friction along the pile than that of a high stiffness pile. Subsequently, using lower stiffness piles could lead to a reduction in carbon heavy materials commonly used for piling (i.e. concrete), and help develop more efficient pile designs.

3 OBJECTIVES

The aim of the test reported in this paper was to compare the capacities of three model piles with varying axial stiffness. The model piles and pile caps were drawn using a 3D modelling software and printed using a Fused Filament Fabrication (FFF) 3D printer.

A geotechnical centrifuge test was undertaken at 50*g* using the facility at City, University of London. During each test the settlement and load was measured for each model pile.

4 MODEL PILES

4.1 3D Printed Piles

A total of three piles were drawn using SolidWorks 3D modelling software and printed using the Markforged Onyx One FFF 3D printer.

FFF 3D printing creates objects by extruding melted plastic or filament through a nozzle and depositing the material layer by layer onto the printing bed. A micro carbon fibre filled nylon filament, known as Markforged Onyx, was used for the model piles in this study as it provides high-strength printed parts.

Due to the limited volume (320x132x154mm) of the printing bed, each model pile was drawn and printed in two halves, with the internal section of the pile faced down on the printing bed, so as to preserve the exterior face roughness from being altered by the printing supports. Each half pile was designed to be 200mm long with an external diameter of 16mm at model scale, which, when accelerated to 50*g* corresponds to a pile with dimensions of 8m long with an outer diameter of 0.8m at prototype scale.

The axial pile stiffness was varied by means of changing the size of the hollow core for each model pile. The preliminary sizes of the hollow cores were chosen to be 3, 6, and 9mmOD, which correspond to piles with an axial stiffness (with a Young's modulus of 2.4kN/mm^2) of 2.33, 2.09, and 1.68 kN/mm, respectively. Comparatively, the stiffness of model piles with equal dimensions made from concrete with a Young's modulus of 25 kN/mm^2 would be 24.29, 21.75, and 17.46 kN/mm respectively. Similarly, for a steel pile with a Young's modulus of 205 kN/mm^2, with identical dimensions, the axial stiffness values would be 209.3, 186.43, and 148.3 kN/mm. To join the two halves of each model pile together, a channel and a ridge were included on the internal side of each half pile wall. Upon printing and removing excess filament from the model piles, each of the two corresponding pile halves were fixed together by applying Araldite epoxy resin to the channels, aligning them so the ridge fits into the channel, clamping the two halves together, and allowing the resin to cure. The bonded model piles are shown in Figure 1.

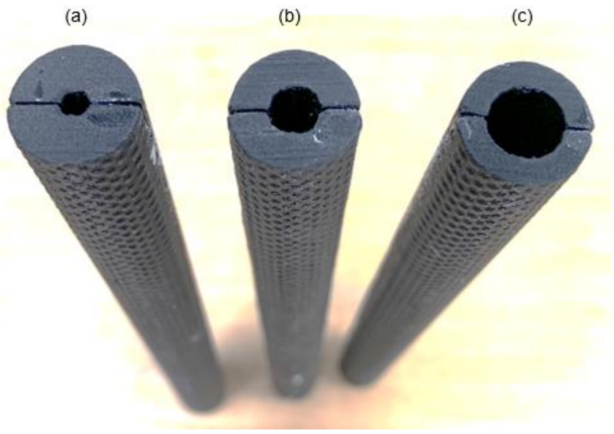

Figure 1: 3D printed piles with hollow cores of (a) 3mmOD (b) 6mmOD (c) 9mmOD

4.2 3D Printed roughness

The use of 3D printed model piles was chosen for this investigation for the benefit of accurate repition of the surface roughness profile for every model pile. Traditional methods of modelling piled foundations using geotechnical centrifuge modelling techniques, such as using steel or aluminium tubes, can be relatively quick and inexpensive. However, unless a roughness was applied to the profile of the model pile it essentially represents a smooth surface – thus reducing the shear resistance at the interface between the model pile and soil.

In order to apply a roughness to model piles, some researchers use methods such as machining a roughness on the model pile surface (O'Hara & Martinez, 2022), or sandblasting or gluing sand to the outside of the model pile (Ouzzine *et al.*, 2023). Although these methods do increase the surface roughness of a pile, it is extremely difficult to replicate the exact roughness profile on all piles used within the test or a series of tests.

Therefore, a built-in 3D texture from the SolidWorks Appearances library was used. Initially, the texture was applied as a 2D pattern on the outside face of the pile, allowing to scale the pattern and set a texture offset distance. A mesh was then applied to the external face of the pile, which, when applied to the preset texture allowed for white areas of the

Table 1: Measured roughness values, R_a, for concrete block and five 3D printed roughness gauge blocks

	Concrete Block	Roughness gauge block offset distance (mm)				
		0.05	0.10	0.15	0.20	0.25
Roughness Value, R_a (μm)	12.06	4.90	7.88	8.79	10.56	11.98

pattern to protrude to the selected texture offset distance, thus creating a rough surface profile when printed. The application of the model pile surface roughness progression is shown in Figure 2.

The texture offset distance was chosen based on testing five roughness gauge blocks which were 3D printed using the same method as for the model piles. The roughness offset distances for the gauge blocks were: 0.05, 0.10, 0.15, 0.20, and 0.25mm. The surface roughness value, R_a, of these blocks was measured using a Mitutoyo Surftest SJ-210 surface roughness measurement instrument. The R_a values of the gauge blocks were then compared to the R_a value of a 100x100x100mm concrete block with a cement to sand to aggregate ratio of 1:2:3. These values are summarised in Table 1.

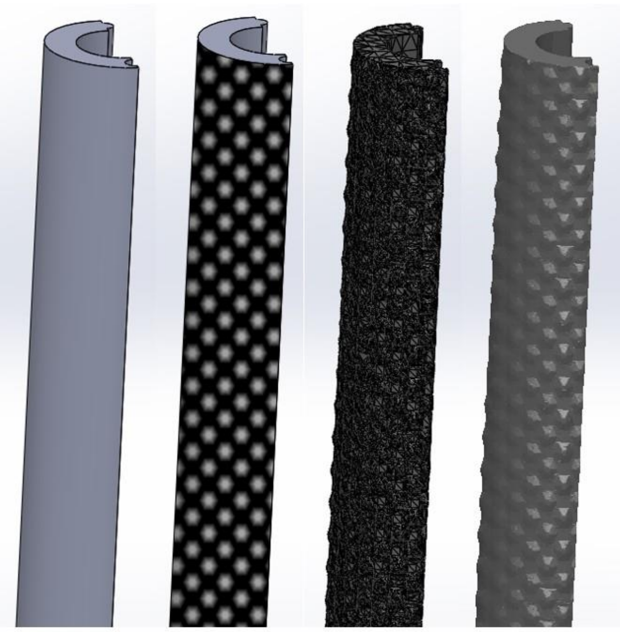

Figure 2: Model pile surface roughness application progression using SolidWorks. (a) Plain pile face (b) Pile face with applied 2D pattern (c) Pile face with applied mesh (d) Pile face with applied mesh, contours removed for clarity

5 SOIL MODEL

The centrifuge test was conducted in a 375mm deep soil container (known herin as a strongbox) with an internal area of 550x220mm. Due to the movement limits of the loading frame, it was necessary to create a soil sample which was 20mm below the top of the strongbox. Therefore, a 300mm deep extension was fitted on top of the strongbox for the consolidation process.

Prior to consolidating the sample, the internal walls of the strongbox and extension were coated with water pump grease in order to minimise friction at the boundaries (Phillips, 1995). The soil used in the test was Speswhite kaolin, which was mixed to a slurry with a water content of 110% by mixing dry powder and distilled water in an industrial ribbon blade mixer. A 3mm thick sheet of porous plastic and filter paper were placed at the base of the strongbox over the herringbone drainage channels to allow free drainage of water from the sample during consolidation. The clay slurry was then carefully placed into the strongbox and extension arrangement whilst being periodically aggitated with a palette knife to ensure that there would be no trapped air bubbles within the sample. Upon reaching the required depth of slurry, another sheet of porous plastic with filter paper was placed on top of the slurry to allow for drainage through holes on the hydraulic press loading platen.

The sample was then transferred to the hydraulic press and consolidated in increments, up to a maximum vertical stress of 500kPa over a period of 10 days, followed by a 1 day swelling period to a vertical stress of 250kPa. This produced a firm yet workable clay sample (Divall & Goodey, 2015; McNamara *et al.*, 2009). During the swelling period, two pore pressure transducers (PPT's) were installed along the centreline of the model through the back face of the strongbox, at depths of 150 and 230mm below the top of the sample.

6 MODEL MAKING

The sample was removed from the consolidation press on the day of testing and prepared for the centrifuge test. The extension was unbolted, removed from the strongbox, and the sample was trimmed to the required height using an aluminium trimming tool with a frame which is supported by the sides of the strongbox, allowing to create a level surface for the soil sample. The model was then prepared under 1*g* conditions.

A PMMA template with a number of evenly spaced holes along the centreline was used as the pile installation guide to determine the exact positions of the model piles within the soil sample, as shown in Figure 3.

Figure 3: Pile installation guide on soil sample

Only three of the sites have been used for this experiment, with aluminium collars mounted on top to provide a pile boring guide, ensuring the bore remains vertical throughout a set pile embedment depth of 180mm at model scale, which equates to 9m at prototype scale when accelerated to 50*g*. A thin-walled hypodermic tube with a 16mmOD was used to cut the bores at a spacing of 165mm c/c.

Upon boring the sample, the model piles were carefully installed into their respective positions and the top of the sample was sprayed with PlastiDip aerosol, a flexible matt coating once dried, to ensure no moisture loss occurs during sample consolidation in-flight.

Once the PlastiDip had dried, the pile caps and ball bearings were carefully placed on top of the piles. The loading frame used for this test, shown in Figure 4, with load cells and Linear Variable Differential Transformerss (LVDT's) pre-attached to align with the positions of the piles and pile caps, was attached to the strongbox and the model was placed on the swing (*Figure 5*). A standpipe was connected to the model which was used to establish a water table situated 10mm below the surface of the ground level. The model was then accelerated to 50*g* and left to consolidate on the swing for approximately 48 hours to ensure any excess pore water pressures had dissipated, which was monitored and confirmed by the PPT's in the sample.

The model piles were then loaded at a rate of 1mm/min, whilst observing the load-settlement response from the centrifuge control room. This loading rate is based on past research conducted by Gorasia (2013), wherein it is stated that a loading rate of 0.25mm/min allows for an undrained loading scenario, hence it is deduced that a loading rate of 1mm/min also ensures undrained loading conditions. The test was completed when the piles reached a settlement of 10mm, which was determined by observing the settlements recorded by the LVDT's.

Once the test had been completed, the model was decelerated and the undrained shear strength profile was measured using a Pilcon hand shear vane.

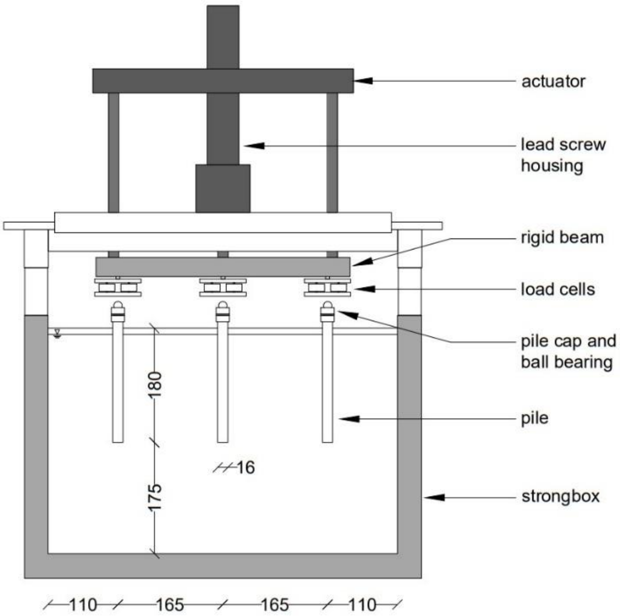

Figure 4: Schematic diagram of model layout

Figure 5: Model and load frame prior to spin up

7 TEST RESULTS

A preliminary test was conducted to determine the effect of varying the stiffness of the pile on its ultimate capacity. The applied load measured on each pile was plotted against the pile displacement normalised by pile diameter (Figure 6).

Figure 6 shows there was a considerable difference between pile capacity at working load (taken as 1% normalised settlement in this study) and ultimate load (10% normalised settlement) between the three piles. Primarily, this relationship could be seen as an increase in pile capacity as a result of the reduction in stiffness.

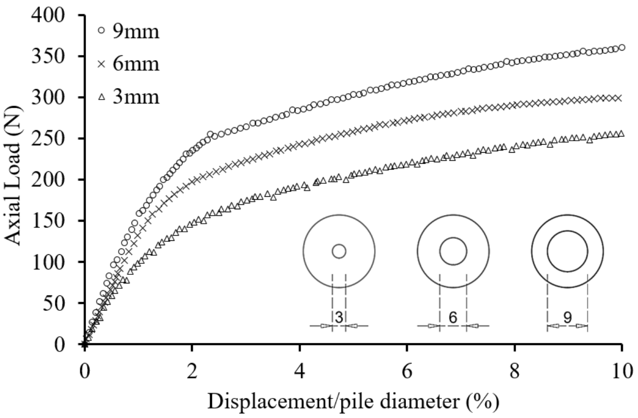

Figure 6: Settlement response for the three test piles from centrifuge test

In addition, the undrained shear strength profile was also estimated using water content samples (after Lalicata *et al*., 2023). The results are shown in Figure 7.

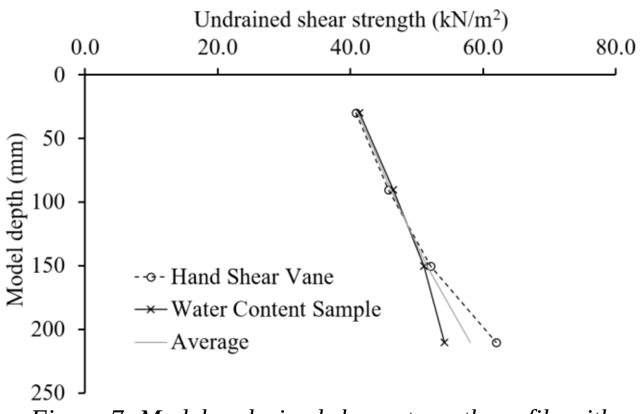

Figure 7: Model undrained shear strength profile with depth

8 RESULT ANALYSIS

Using the principle of Terzaghi (1943), pile capacity, Q, is the sum of shaft and base capacity (Q_s and Q_b respectively), which can be determined using the following equations:

$$Q = Q_{shaft} + Q_{base} \quad (1)$$

$$Q_s = A_{shaft}\, \alpha\, S_{u(ave)} \quad (2)$$

$$Q_b = A_{base}(N_c S_u + \gamma H) \quad (3)$$

Where A (m^2) is the area of the shaft or base of the model pile, α is the dimensionless adhesion factor, *Su* (kN/m^2) is the undrained shear strength of the soil, N_c is the dimensionless bearing capacity factor, γ (kN/m^3) is the bulk unit weight of the soil, and H (m) is the embedment depth of the model pile. These values are summarised in Table 2. For the purpose of this test, it is assumed that the end bearing capacity for all three piles is equal (see Table 2) as they have identical base geometry.

Table 2: Properties used for back analysis of test results

Property	Value	Units
γ	17.44	kN/m^3
$Su_{(ave)}$	49.2	kN/m^2
$Su_{(base)}$	54.9	kN/m^2
H	0.18	m
N_c ($^L/_B$ >>4)	9	-
A_{base}	0.000201	m^2
A_{shaft}	0.0094	m^2
Q_b	0.0178	kN

Table 3 gives the shaft capacity values, which have been back-calculated to give adhesion factors for each pile at ultimate capacity (i.e., 10% normalised displacement). It should be noted that the load settlement curves suggest that the pile capacity has not yet reached the limit value yet, therefore, the estimated alpha values represent a lower limit. The results confirm higher adhesion factors between the soil and the piles with lower axial stiffness values due to additional straining along the embedment length of the pile – thus an increase in the mobilisation of the undrained shear strength of the soil as the pile displaces. Similar results were also observed by Panchal et al. (2019).

Table 3: Summary of alpha values at ultimate capacity

Annulus diameter (mm)	Axial stiffness (kN/mm)	Load (kN)	Q_s (kN)	α
3	2.33	0.26	0.24	0.52
6	2.09	0.30	0.28	0.61
9	1.68	0.36	0.34	0.74

9 CONCLUSIONS AND FUTHER WORK

A preliminary centrifuge test was undertaken at 50*g* to compare the behaviour of three piles with a varying axial stiffness under an applied load.

The results support the theory that piles with lower values of axial stiffness mobilise a higher portion of the undrained shear strength of the soil due to increased strains along the length of the pile, as opposed to piles with higher values of axial stiffness. The increased strains in turn increase the shaft friction, thus providing piles with a higher ultimate capacity at working load.

A further series of tests, as part of a parametric study, are to follow on from this preliminary test. Future work will aim to test a larger range of piles with varying values of axial stiffness, as well as monitoring the strains along the length of the pile in order to gain a better understanding into how the increased strains under an applied load affect the capacity of the pile.

REFERENCES

Burland, J.B., 2023. Behaviour of single piles under vertical loads. In *ICE Manual of Geotechnical Engineering, Second edition, Volume I: Geotechnical engineering principles, problematic soils and site investigation* (pp. 257-272). Emerald Publishing Limited. https://doi.org/10.1680/icemge.66816.0257

Divall, S. and Goodey, R.J., 2015. Twin-tunnelling-induced ground movements in clay. *Proceedings of the Institution of Civil Engineers-Geotechnical Engineering*, *168*(3), pp.247-256. https://doi.org/10.1680/geng.14.00054

Gorasia, R.J., 2013. Behaviour of ribbed piles in clay (Doctoral dissertation, City University London).

Lalicata, L.M., Stallebrass, S.E. and McNamara, A., 2023. An experimental study into the ultimate capacity of an 'impression'pile in clay. *Géotechnique*, *73*(5), pp.455-466. https://doi.org/10.1680/jgeot.21.00168

McNamara, A.M., Goodey, R.J. and Taylor, R.N., 2009. Apparatus for centrifuge modelling of top down basement construction with heave reducing piles. *International Journal of Physical Modelling in Geotechnics*, *9*(1), pp.01-14. https://doi.org/10.1680/ijpmg.2009.090101

O'Hara, K.B. and Martinez, A., Shaft and Base Capacity of Snakeskin-Inspired Piles from Centrifuge Pile Tests. In *Geo-Congress 2022* (pp. 170-180).

Ouzzine, B., de Sauvage, J., Madabhushi, G., Viggiani, G. and Reiffsteck, P., 2023. Centrifuge modelling of an energy pile group with ground water flow. *International Journal of Physical Modelling in Geotechnics*, pp.1-25. https://doi.org/10.1680/jphmg.22.00041

Panchal, J.P., McNamara, A.M., Halai, H. and Divall, S., 2019, September. Centrifuge modelling to determine the influence of pile stiffness on pile capacity. In *Proceedings of the XVII European Conference on Soil Mechanics and Geotechnical Engineering*. International Society for Soil Mechanics and Geotechnical Engineering.

Phillips R (1995) Centrifuge modelling: practical considerations. In *Geotechnical Centrifuge Technology* (Taylor RN (ed.)).

Terzaghi, K. 1943. Theoretical Soil Mechanics, John Wiley and Sons, New York.In *Piling 2020: Proceedings of the Piling 2020 Conference* (pp. 193-198). ICE Publishing.